Efficient High Area OFETs by Solution Based Processing of a π−Electron Rich Donor

ARTICLE *in* CHEMISTRY OF MATERIALS · OCTOBER 2006

Impact Factor: 8.35 · DOI: 10.1021/cm060675m

Articles

Efficient High Area OFETs by Solution Based Processing of a π-Electron Rich Donor

Pawel Miskiewicz,[†] Marta Mas-Torrent,[‡] Jaroslaw Jung,[†] Sylwia Kotarba,[†] Ireneusz Glowacki,[†] Elba Gomar-Nadal,[‡] David B. Amabilino,[‡] Jaume Veciana,[‡] Bärbel Krause,[§] Dina Carbone,[§] Concepció Rovira,*[,‡] and Jacek Ulanski*[,†]

Department of Molecular Physics, Technical University of Lodz, 90-924 Lodz, Poland, Institut de Ciència de Materials de Barcelona (CSIC), Campus Universitari de Bellaterra, 08193 Cerdanyola del Vallès, Spain, and European Synchrotron Radiation Facility, ESRF BP 220 F-38043, Grenoble Cedex, France

Received March 21, 2006. Revised Manuscript Received June 30, 2006

We report on the preparation of high performance field-effect transistors (FETs) based on large areas of aligned films of a TTF derivative, namely, tetrakis-(octadecylthio)-tetrathiafulvalene (TTF-4SC18). TTF-4SC18 assembles into one-dimensional stacks in which the long alkyl chains promote intermolecular $\pi-\pi$ overlapping due to their extremely closely packed nature. The films were prepared from solution by zone-casting, a simple technique that does not require the use of preoriented substrates. The films were characterized by AFM and X-ray, indicating an extremely high crystalline quality. The TTF molecules are tilted with respect to the substrate surface and are well-aligned in the casting direction. More than 40 FETs were measured, showing a remarkable reproducibility of their performance. The average charge carrier mobility value measured along the casting direction was about 0.006 cm^2/V s for a channel length $L = 100$ μm and about 0.01 cm^2/V s for $L = 80$ μm and $L = 50$ μm. The FET mobilities determined in the direction perpendicular to the orientation were ca. 1 order of magnitude lower. We found that all the devices after annealing exhibited an enhanced performance with FETs mobilities about 1 order of magnitude higher. The best devices revealed a charge carrier mobility close to 0.1 cm^2/V s with an on/off ratio of the order of 10^4.

Organic molecules containing conjugated π systems have been the subject of basic research for many years owing to their interesting optical and electronic properties. Nevertheless, it is only in the past decade that these materials have attracted increasing interest due to their potential applications as active layers in devices such as photovoltaic cells, light emitting diodes, and field-effect transistors (FETs). FETs with sufficient performance for industrial manufacturing have already been fabricated employing organic semiconductors.[1,2] However, one of the main problems limiting broader exploitation of these materials is their processability. Most organic semiconductors that exhibit high charge carrier mobilities show poor solubility in organic solvents, and therefore, vacuum techniques,[3] precursor routes,[4−7] or friction transfer methods[8] are often required for processing them. In this respect, tetrathiafulvalene (TTF) and its derivatives[9] are excellent candidate materials due to their high FET performance and facile processability either under vacuum or from solution.[10,11] A second added hindrance for industrial application of organic FETs is the lack of efficient low-cost methods for aligning the organic molecules in such a way that the electronic transport would be parallel to the substrate with in-plane electrodes in a FET configuration.[2] To control and optimize the structural organization of the organic molecules, which determines the efficiency of the charge transport, studies on the influence of the substrate temperature on the molecular arrangement in FETs fabricated by evaporation have been performed.[12,13] By chemical modification of the molecular cores, it is also possible to gain control

* Corresponding authors. (C.R.) E-mail: cun@icmab.es; tel.: +34 935801853; fax: +34 935805729. (J.U.) E-mail: Jacek.Ulanski@p.lodz.pl; tel: +48 426313205; fax: +48 42 6313218.
[†] Technical University of Lodz.
[‡] Institut de Ciència de Materials de Barcelona.
[§] European Synchrotron Radiation Facility.

(1) Sun, Y. M.; Liu, Y. Q.; Zhu, D. B. *J. Mater. Chem.* **2005**, *15*, 53.
(2) Dimitrakopoulos, C. D.; Malenfant, P. R. L. *Adv. Mater.* **2002**, *14*, 99.
(3) Dimitrakopoulos, C. D.; Purushothaman, S.; Kymissis, J.; Callegari, A.; Shaw, J. M. *Science* **1999**, *283*, 822.
(4) Afzali, A.; Dimitrakopoulos, C. D.; Breen, T. L. *J. Am. Chem. Soc.* **2002**, *124*, 8812.
(5) Murphy, A. R.; Fréchet, J. M. J.; Chang, P.; Lee, J.; Subramanian, V. *J. Am. Chem. Soc.* **2004**, *126*, 1596.
(6) Herwig, P. T.; Müllen, K. *Adv. Mater.* **1999**, *11*, 480.
(7) Gelink, G. H. et al. *Nat. Mater.* **2004**, *3*, 106.
(8) Nagamatsu, S.; Takashima, W.; Kaneto, K.; Yoshida, Y.; Tanigaki, N.; Yase, K.; Omote, K. *Macromolecules* **2003**, *36*, 5252.
(9) See papers in the issue of *Chem. Rev.* **2004**, *104*.
(10) Mas-Torrent, M.; Rovira, C. *J. Mater. Chem.* **2006**, *16*, 433.
(11) (a) Noda, B.; Katsuhara, M.; Aoyagi, I.; Mori, T.; Taguchi, T. *Chem. Lett.* **2005**, *34*, 392. (b) Katsuhara, M.; Aoyagi, I.; Nakajima, H.; Mori, T.; Kambayashi, T.; Ofuji, M.; Takanishi, Y.; Ishikawa, K.; Takezoe, H.; Hosono, H. *Synth. Met.* **2005**, *149*, 219. (c) Naraso; Nishida, J.-I.; Ando, S.; Yamaguchi, J.; Itaka, K.; Koinuma, H.; Tada, H.; Tokito, S.; Yamashita, Y *J. Am. Chem. Soc.* **2005**, *127*, 10142.

10.1021/cm060675m CCC: $33.50
Published on Web 09/02/2006

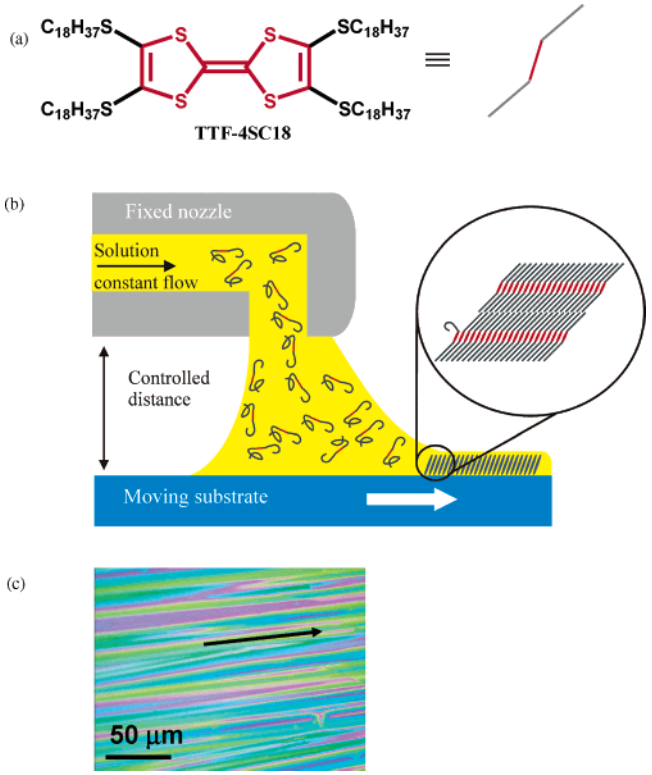

Figure 1. (a) Molecular structure of tetrakis-(octadecylthio)-tetrathiafulvalene (TTF-4SC18). (b) Schematic representation of the zone-casting technique. (c) Optical micrograph image of the TTF-4SC18 zone-cast film. The black arrow indicates the casting direction.

over the resulting film order.[14−16] An alternative recent approach employed for soluble semiconductors has focused on the utilization of preoriented substrates, combining in this way high interfacial order and solution processing.[17]

In this paper, we report on the preparation of FETs based on large areas of highly oriented films of a soluble TTF derivative, tetrakis-(octadecylthio)-tetrathiafulvalene (TTF-4SC18), obtained by the so-called zone-casting technique, a one-step method for preparing large area oriented films of solution-processible materials with no need to use a preoriented substrate (Figure 1). The devices prepared with these films revealed a remarkably high performance, with a maximum charge carrier mobility close to 0.1 cm^2/V s.

TTFs are relatively easily functionalized,[18] affording variable solubility according to the type, number, and position of the substituents and the possibility of tuning their electronic and structural properties. We recently reported that there is a strong correlation between crystal structure and device performance in FETs based on single crystals of TTFs, which was further corroborated by calculations.[19,20] The highest mobilities were found in single crystals of TTF molecules crystallizing in one-dimensional stacks (i.e., dithiophene-TTF, $\mu_{max} = 1.4$ cm^2/V s[21] and dibenzo-TTF, $\mu_{max} = 1$ cm^2/V s[22]). Interestingly, for low-cost electronics, all these crystals were grown from solution. However, to move toward applications, it is imperative to develop easy methods to prepare crystalline films for large area coverage. For this purpose, we studied the derivative TTF-4SC18 (Figure 1a), which was prepared using the known procedure.[23] Related compounds of this type, which assemble into one-dimensional segregated stacks of TTF units and alkyl chains, show conductivities of 10^{-5} S cm^{-1} as single crystals.[24] This high one-dimensional electrical conduction for a nondoped molecular crystal is attributed to the intermolecular $\pi-\pi$ overlapping caused by the extremely closely packed nature of the long alkyl chains. Taking all this into consideration, TTF-4SC18 seems to be a promising material for the preparation of crystalline films by zone-casting for fabricating FETs since the long alkyl chains might promote the formation of high quality ordered films in which the TTF cores, responsible for the electronic properties, will be densely packed.

The zone-casting technique, which consists of supplying a solution of an organic material through a stationary flat nozzle onto a moving substrate, was originally designed to produce composites of conducting polymers and quasi-one-dimensional organic metals, like charge-transfer complexes of 7,7′,8,8′-tetracyanoquinodimethane with tetrathiotetracene or TTF. These composites showed very high optical as well as direct current and alternate current conductivity anisotropy.[25] Recently, this method has been successfully adapted to produce oriented layers of the discotic liquid crystal molecule hexa(*n*-dodecyl)hexa-peri-benzo-coronene for FET devices.[26−28]

Results and Discussion

Large area films (3 cm × 10 cm) of TTF-4SC18 on a $SiO_2/Si_3N_4/Si$ substrate were obtained from a toluene solution using the originally designed zone-casting apparatus (Figure

(12) Dimitrakopoulos, C. D.; Mascaró, D. J. *IBM J. Res. Dev.* **2001**, *45*, 11.
(13) Locklin, J.; Li, D.; Mannsfeld, S. C. B.; Borkent, E.-J.; Meng, H.; Advincula, R.; Bao, Z. *Chem. Mater.* **2005**, *17*, 3366.
(14) Curtis, M. D.; Cao, J.; Kampf, J. *J. Am. Chem. Soc.* **2004**, *126*, 4318.
(15) Halik, M.; Klauk, H.; Zschieschang, U.; Schmid, G.; Ponomarenko, S.; Kirchmeyer, S.; Weber, W. *Adv. Mater.* **2003**, *15*, 917.
(16) Li, Y.; Wu, Y.; Gardner, S.; Ong, B. S. *Adv. Mater.* **2005**, *17*, 849.
(17) Van de Craats, A. M.; Stutzmann, N.; Bunk, O.; Nielsen, M. M.; Watson, M.; Mullen, K.; Chanzy, H. D.; Sirringhaus, H.; Friend, R. *Adv. Mater.* **2003**, *15*, 495.
(18) Yamada, J.; Sugimoto, T. *TTF Chemistry*; Kodansha Ltd., and Springer-Verlag: Tokyo and Berlin, 2004.
(19) Mas-Torrent, M.; Hadley, P.; Bromley, S. T.; Mas, M.; Molins, E.; Ribas, X.; Tarrés, J.; Veciana, J.; Rovira, C. *J. Am. Chem. Soc.* **2004**, *126*, 8546.
(20) Bromley, S. T.; Mas-Torrent, M.; Hadley, P.; Rovira, C. *J. Am. Chem. Soc.* **2004**, *126*, 6544.
(21) Mas-Torrent, M.; Durkut, M.; Hadley, P.; Ribas, X.; Rovira, C. *J. Am. Chem. Soc.* **2004**, *126*, 984.
(22) Mas-Torrent, M.; Hadley, P.; Bromley, S. T.; Crivillers, N.; Veciana, J.; Rovira, C. *Appl. Phys. Lett.* **2005,** *86*, 012110.
(23) Wu, P.; Saito, G.; Imaeda, K.; Shi, Z.; Mori, T.; Enoki, T.; Inokuchi, H. *Chem. Lett.* **1986**, 441.
(24) Inokuchi, H.; Saito, G.; Wu, P.; Seki, K.; Tang, T. B.; Mori, T.; Imaeda, K.; Enoki, T.; Higuchi, Y.; Inaka, K.; Yasouka, N. *Chem. Lett.* **1986**, 1263.
(25) Burda, L.; Tracz, A.; Pakula, T.; Ulanski, J.; Kryszewski, M. *J. Phys. D: Appl. Phys.* **1983**, *16*, 1737. (b) Ulanski, J.; Tracz, A.; El Shafee, E.; Debrue, G.; Deltour, R. *Synth. Met.* **1990**, *35*, 221. (c) Tracz, A.; El Shafee, E.; Ulanski, J.; Jeszka, J. K.; Kryszewski, M. *Synth. Met.* **1990**, *37*, 175.
(26) Miskiewicz, P.; Rybak, A.; Jung, J.; Glowacki, I.; Ulanski, J.; Geerts, Y.; Watson, M.; Müllen, K. *Synth. Met.* **2003**, *137*, 905.
(27) Miskiewicz, P. et al. First demonstration of FET devices made by zone-casting techniques, presented at the UE project DISCEL annual meeting, Mainz, Germany, March 10−11, 2003.
(28) Pisula, W.; Menon, A.; Stepputat, M.; Lieberwirth, I.; Kolb, U.; Tracz, A.; Sirringhaus, H.; Pakula, T.; Müllen, K. *Adv. Mater.* **2005**, *17*, 684.

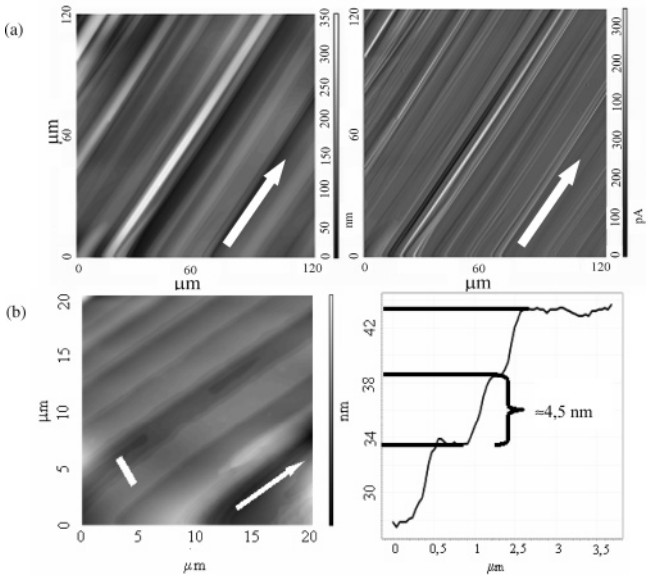

Figure 2. (a) AFM height (left) and amplitude (right) images of the zone-cast layer of TTF-4SC18. (b) Magnified AFM height image of the zone-cast TTF-4SC18 film (left) and profile of the surface (right) along the white bar shown in the left image. The arrows indicate the casting direction.

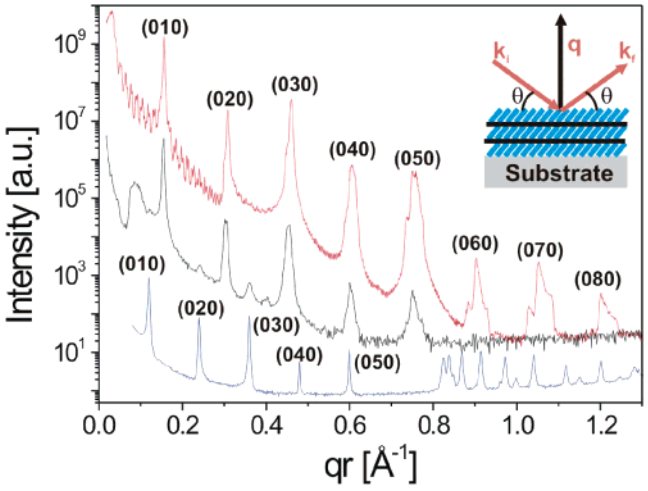

Figure 3. X-ray reflectivity scan (red line) and offset scan (0.2° shifted to the specular direction, black line) obtained of the zone-cast layer of TTF-4SC18. For comparison, a powder diffraction spectrum of the TTF-derivative is shown (blue line). The inset shows the scattering geometry of the reflectivity measurement.

1b) in which substrate and nozzle were thermally stabilized independently. Figure 1c shows an optical microscope image of the films obtained in which continuous large and long crystalline stripes following the casting direction can be observed due to the tendency of TTF-4SC18 to crystallize unidirectionally in the applied zone-casting conditions. We assume that during the evaporation of the solvent in the meniscus, some crystallites are formed with arbitrary orientation in the substrate plane. The preferential orientation of the crystallites is subsequently established from the growth competition between them. The crystallites oriented with the stacking axis in the casting direction grow more rapidly since this is the preferential growth direction of the crystals (i.e., stronger intermolecular interactions) and, in addition, corresponds also to the direction in which there is a continuous supply of molecules (Figure 1b).[29]

Inspection of the films by AFM (Figure 2a) demonstrates that the surface of the crystalline films is highly smooth in the casting direction, while in the perpendicular direction terraces of several micrometers in width, with step heights of ca. 4−5 nm, have been formed (Figure 2b). The crystalline structure of the film was also studied by X-ray diffraction. Reflectivity measurements were performed parallel and perpendicular to the casting direction, at different positions on the sample separated by up to 30 mm. The experiments were highly reproducible, supporting the hypothesis of long-range homogeneity and high crystalline ordering of the TTF-4SC18 films. The X-ray reflectivity measurement (see Figure 3, red line) shows the (010) Bragg reflection at $q = 0.150$ Å^{-1} and its higher orders (0n0) up to $n = 8$, corresponding to $b = 41.8$ Å. This distance is in agreement with the steps observed by AFM and also points out that the TTF-4SC18 molecules are arranged with their long axis oblique to the surface. Therefore, the molecular stacking direction that forms the conduction channel is parallel to the substrate, which is a crucial requirement for the preparation of FETs. The presence of this large number of reflections of orders greater than (010) and the width $\Delta q = 0.0035 \pm 0.0005$ Å^{-1} of the (010) Bragg peak is also an indication of a highly ordered crystalline film, which has a thickness of $D = 180 \pm 30$ nm. It is worth noting that the higher orders of the (010) reflection show a peak splitting that might be related to the coexistence of several polymorphs with a slightly different crystalline structure. The mosaicity of the film perpendicular to the substrate was smaller than the experimental resolution of 0.01°. Additionally, measurements of the diffuse scattering with an offset of 0.1° with respect to the specular direction were also performed (Figure 3, black line). The intensity of the diffuse scattering is 3 orders of magnitude lower than the specular scattering, indicating the low degree of disorder within the molecular layers and the low degree of roughness at the surface of the film. An intensity enhancement was found close to the Bragg peaks. These are the so-called Bragg sheets and indicate the strong correlation of imperfections in subsequent molecular layers, which are transferred from one molecular layer to the next. Bragg sheets are also observed for other lamellar molecular systems with alkane chains, including stacked lipid membranes and Langmuir−Blodgett films.[30−32] For comparison, we also measured the powder diffraction spectrum (Figure 3, blue line), and we observed that the (0n0) Bragg peaks were clearly shifted with respect to the peaks found in the reflectivity measurements. This indicates that the film structure deviates from the bulk crystalline structure, and therefore, the zone-casting process has a strong influence on the crystalline structure, probably due to the influence of the substrate on the nucleation process and/or the control of the evaporation process.

(29) Rodriguez-Navarro, A.; Garcia-Ruiz, J. M. *Eur. J. Mineral.* **2000**, *12*, 609.

(30) Nitz, V.; Tolan, M.; Schlomka, J. P.; Seeck, O. H.; Stettner, J.; Press, W.; Stelzle, M.; Sackmann, E. *Phys. Rev. B* **1996**, *54*, 5038.
(31) Salditt, T. *J. Phys. Condens. Matter* **2005**, *17*, R287.
(32) Gibaud, A.; Cowlam, N.; Vignaud, G.; Richardson, T. *Phys. Rev. Lett.* **1995**, *74*, 3205.

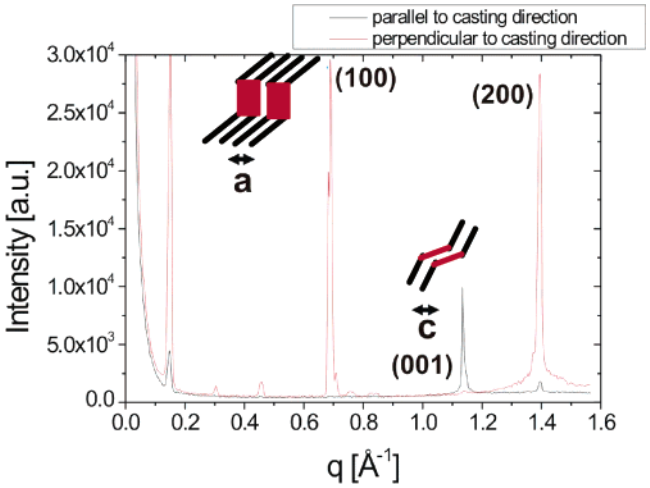

Figure 4. GID radial scans in the casting direction (black line) and perpendicular to it for the zone-cast layer of TTF-4SC18. The characteristic in-plane Bragg peaks are indicated, as well as a model for the molecular arrangement in the respective directions. The inset schemes represent the geometry of neighboring molecules that consist of a central TTF core (in red) with alkyl chains (in black).

Figure 4 shows radial measurements in grazing incident diffraction (GID) geometry. In the casting direction, a (001) Bragg peak at $q = 1.134$ Å^{-1}, corresponding to the lattice parameter $c = 5.5$ Å, is observed. Perpendicular to the casting direction, this peak is nearly completely suppressed. Instead, strong (100) and (200) reflections at $q = 0.690$ Å^{-1} are observed, corresponding to a lattice parameter $a = 9.1$ Å. The observation of different Bragg peaks in the casting direction and perpendicular to it demonstrates that the film is azimuthally oriented. The azimuthal distribution (studied keeping q fixed at the (100) and (001) Bragg peaks and measuring the intensity as a function of the azimuthal orientation of the sample) was found to be $\Delta\omega = 10°$. Because of the extremely large size of the crystallites, this distribution is inhomogeneous and consists of many extremely sharp intensity spikes (not shown). Measurements repeated at several positions on the sample confirm the reproducibility of these observations. The unit cell of the organic thin film is found to be orthorhombic with one molecule per unit cell and the lattice parameters $a = 9.1$ Å, $b = 41.8$ Å, and $c = 5.5$ Å. Because of the small number of measured Bragg peaks, a triclinic distortion of a few degrees cannot be excluded. Taking into account the geometry of the molecule, we propose the following model for the arrangement of the molecules in the film: in the casting direction, where the smallest lattice parameter has been found, the molecules form closely packed molecular wires, permitting high overlapping of the π orbitals. These molecular stacks are laterally and vertically closely packed and well-ordered. The lattice parameter perpendicular to the substrate surface is much smaller than the molecular size of about 53 Å. Since the molecular chains must be closely packed to allow for the observed high crystalline quality, they can be assumed to be straight. Taking into account a possible tilt of the chains with respect to the TTF core, the tilt of the molecule with respect to the substrate can be estimated to be approximately $55 \pm 10°$.

We prepared top contact FETs in such a way that the channel length ($L = 100$, 80, and 50 μm) was parallel to the

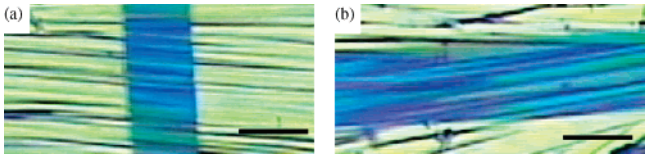

Figure 5. Optical micrographs of the FETs fabricated with the TTF-4SC18 zone-cast layer with the evaporated top gold electrodes, with channels parallel (a) and perpendicular (b) to the casting direction; scale bar is 80 μm.

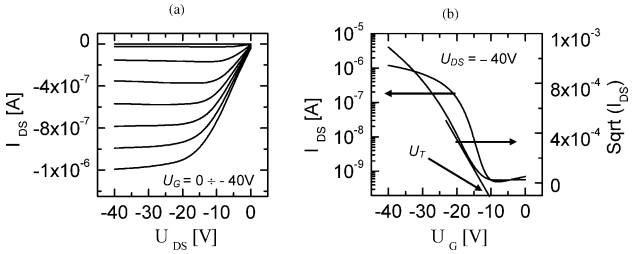

Figure 6. Output (a) and transfer (b) characteristics of FET based on the zone-cast TTF-4SC18 layer with the channel length parallel to the casting direction on the $SiO_2/Si_3N_4/Si$ substrate with $W = 2$ mm and $L = 100$ μm. The output characteristics were measured for the gate voltage U_G in the range of 0 to −40 V. The charge carrier mobility calculated for this device was 0.009 cm^2/V s.

casting direction (Figure 5a). We also prepared several FETs with a channel length ($L = 80$ μm) perpendicular to the casting direction (Figure 5b). The bottom Si contact was used as the gate electrode. The output I_{DS} versus U_{DS} and transfer I_{DS} versus U_G characteristics of a device with a channel length of 100 μm and a channel width of 2 mm are depicted in Figure 6 (where I_{DS} is the current flowing between the drain and the source for a given gate voltage (U_G) and source-drain voltage (U_{DS})). These curves are typical for *p*-type field-effect transistors since as a more negative gate voltage is applied, more holes are induced in the conduction channel and the source-drain current increases. The charge carrier mobility (μ_{FET}) of the investigated devices was calculated from the saturation regime (for details, see Experimental Procedures). More than 40 FETs were produced and tested, showing a remarkable reproducibility in their performance. The mobilities obtained for all these devices are depicted in Figure 7a. For the devices with the channel parallel to the casting direction, the average charge carrier mobility value μ_{FET} was about 0.006 cm^2/V s for the devices with channel length $L = 100$ μm and $\mu_{FET} = 0.01$ cm^2/V s for the ones with $L = 80$ μm and $L = 50$ μm. For all these devices, the on/off ratio was in the range of 10^3 to 10^4, and the threshold voltage (U_T) was between −6 and − 10 V. The best device exhibited a mobility of 0.015 cm^2/V s and an on/off ratio of ca. 10^4. For the devices with the channel perpendicular to the casting direction, the average mobility was 0.0017 cm^2/V s, and the on/off ratio was in the range of 10^2 to 10^4 with $U_T = -15$ to −20 V. Such a relatively low anisotropy of the charge mobility as compared with results reported for other FETs obtained with different oriented organic layers[33,34] may arise from the geometry and relatively large sizes of the channel lengths and widths. As one can see in Figure

(33) Linda Chen, X.; Lovinger, A. J.; Bao, Z.; Sapjeta, J. *Chem. Mater.* **2001**, *13*, 1341
(34) Li, S. P.; Newsome, C. J.; Russell, D. M.; Kugler, T.; Ishida, M.; Shimoda, T. *Appl. Phys. Lett.* **2005**, *87*, 062101.

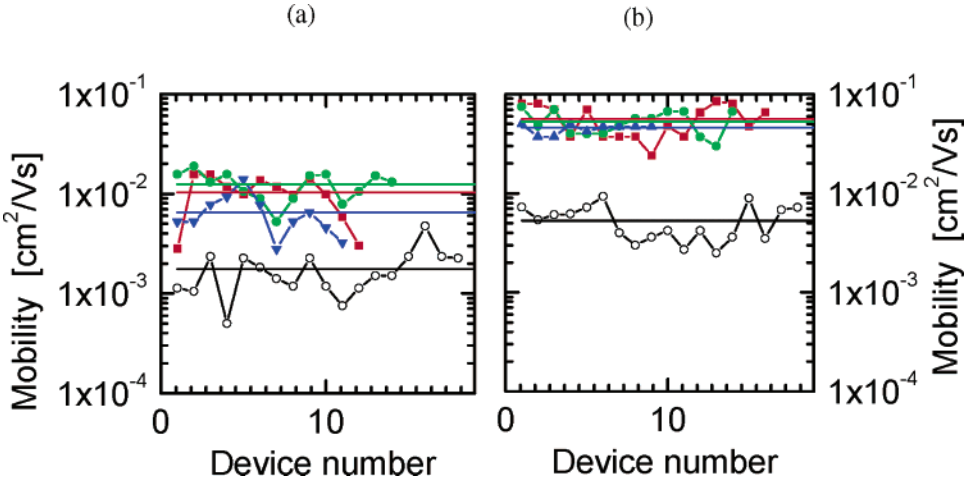

Figure 7. Field-effect mobilities for series of FET devices based on the zone-cast TTF-4SC18 layers on the SiO_2/Si_3N_4/Si substrate with different channel lengths oriented parallel and perpendicular to the casting direction before annealing (a) and after annealing (b). Full symbols show results for the devices with the channel length parallel to the casting direction: squares − $L = 100$ μm, circles − $L = 80$ μm, and triangles − $L = 50$ μm. Open circles show results for the devices with channel length perpendicular to the casting direction, $L = 80$ μm.

5b, the crystalline ribbons forming the oriented layer are not exactly parallel to each other, and even in the devices with channels perpendicular to the casting direction, some ribbons are slightly oblique to the electrode edges, so that for sufficiently large channel widths, they can interconnect both source and drain electrodes.

Since it is well-known that annealing can induce self-healing of organic semiconductors and diminish the density of defects existing at intergrain boundaries and at interfaces with electrodes, the devices were subjected to annealing (for details, see Experimental Procedures). We found that for all the annealed samples, their FET performance improved significantly. All the mobilities obtained for the annealed devices are collected in Figure 7b. For the devices with the channel oriented parallel to the casting direction, the μ_{FET} values increased almost 10 times after annealing for the FETs with $L = 100$ μm and ca. 5 times for the FETs with $L = 50$ and 80 μm. For the devices with channels oriented perpendicular to the casting direction, the average μ_{FET} values increased from 1.7×10^{-3} to 5.3×10^{-3} cm^2/V s. Comparing Figure 7a,b, one can see that the anisotropy of the charge transport becomes more pronounced after the annealing process. Figure 7 also demonstrates that the thermal treatment not only increases the average mobility but also decreases the scattering of the obtained mobility values for different channel lengths. Moreover, after annealing, the mobility is almost independent of the channel length. No noticeable changes in the morphology of the zone-cast layers were observed by AFM and optical microscopy after annealing. As an example, Figure 8 shows the output and transfer characteristics after annealing the device presented in Figure 6. The best device revealed a high charge carrier mobility of 0.08 cm^2/V s with an on/off ratio of the order of 10^4.

Conclusion

In summary, we have prepared high performance FETs based on large area aligned layers of a TTF derivative with long alkyl chains from solution by the zone-casting technique. The X-ray diffraction measurements on the zone-cast layers show an extremely high crystalline quality and indicate

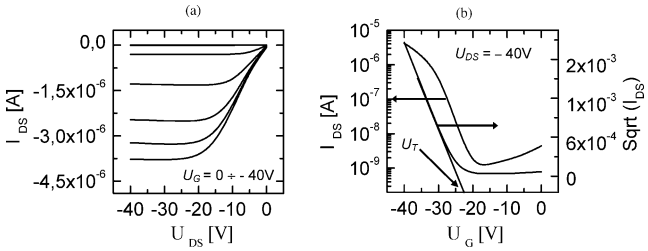

Figure 8. Output (a) and transfer (b) characteristics of FET based on the annealed zone-cast TTF-4SC18 layer with the channel length parallel to the casting direction on the SiO_2/Si_3N_4/Si substrate with $W = 2$ mm and $L = 100$ μm. The output characteristics were measured for the gate voltage U_G in the range of 0 to −40 V. The charge carrier mobility calculated for this device was 0.06 cm^2/V s.

that the TTF molecules are tilted with respect to the substrate surface and are well-aligned in the casting direction. The FET devices can be fabricated in a reproducible way. In addition, it was observed that by annealing the devices, the charge carrier mobility improved significantly, showing a maximum charge carrier mobility close to 0.1 cm^2/V s with an on/off ratio of the order of 10^4.

Experimental Procedures

TTF derivative TTF-4SC18 was synthesized as previously described.[23] Oriented layers of TTF-4SC18 were obtained using originally designed zone-casting apparatus. A 2 mg/mL solution of TTF-4SC18 in toluene was continuously supplied through the stationary flat nozzle onto a moving substrate with a speed of around 25 μm/s. Substrate and nozzle were independently thermally stabilized at 80 and 75 °C, respectively. The dimensions of the TTF-4SC18 layers obtained in this way were 3 cm × 10 cm. Highly doped *n*-type silicon wafers were used as a substrate with 100 nm Si_3N_4 followed by 50 nm SiO_2 as a dielectric layer, both obtained by a plasma enhanced chemical vapor deposition method (Wafernet, San Jose, CA). The surface of the substrate was cleaned with $CHCl_3$ and then isopropyl alcohol and dried with N_2. All samples were dried in a nitrogen atmosphere at 25 °C for 24 h before further investigations. AFM images were taken with a SOLVER PRO scanning probe microscope (NT-MDT, Russia) in resonant mode. The X-ray diffraction experiments were performed at the beamline ID01 of the European Synchrotron Radiation Facility (ESRF) at an X-ray energy of 19.5 keV, corresponding to a wavelength of λ

= 0.636 Å. Radial ($\theta/2\theta$) and angular (ω) scans were performed in a specular direction (reflectivity scans), sensitive to the crystalline ordering of the organic thin film perpendicular to the substrate surface, and in grazing incidence diffraction (GID) geometry (in-plane), sensitive to the crystalline ordering of the film parallel to the substrate surface. The scattering geometry of the reflectivity measurement is shown in the inset of Figure 5. For all measurements, the measured intensity is plotted as a function of the scattering vector $q = \boldsymbol{k}_f - \boldsymbol{k}_i$, where $\boldsymbol{k}_i$ and $\boldsymbol{k}_f$ are the wave vector of the incoming and scattered X-ray beam. Radial scans are measurements where the length of q is varied but its orientation with respect to the sample is fixed. They give information about the lattice spacing d observed in the selected direction. The parameter d is related to the scattering vector by $q = 2\pi/d$. Angular scans are measurements where q is fixed but its orientation with respect to the sample is varied, giving information about the orientation distribution of the crystallites. Additionally, a powder diffraction spectrum of polycrystalline TTF-4SC18 obtained from a toluene solution was recorded as a reference to the bulk crystalline structure. Top contact FETs were prepared by vacuum evaporation of 150 nm thick gold electrodes through a shadow mask. The electrode evaporation was performed at vacuum $<5 \times 10^{-6}$ mbar, with the evaporation rate <0.5 nm/s, so that the temperature of the substrate did not exceeded 40 °C. Devices had channel lengths of 100, 80, and 50 μm and a width of 2 mm for a channel parallel to the casting direction and a length of 80 μm (width of 1.5 mm) for a channel perpendicular to the casting direction. The annealing procedure was performed by keeping the FET devices in dry nitrogen at a lowered pressure (2 mbar) at 65 °C (16 °C below a solid−solid phase transition and 20 °C below the melting point[35]) for 72 h. FETs characteristics were taken using two Keithley 2400 source-measure units for voltage applying and current monitoring in the following way: output characteristics were taken with s step of 5 V in the range of 0 to − 40 V (U_{DS}) for gate voltage (U_G) varying from 0 to − 40 V with a step of 5 V; transfer characteristics were measured at $U_{DS} = -40$ V for the gate voltage varying from 0 to − 40 V with a step of 5 V. The charge carrier mobility (μ_{FET}) of the investigated devices was calculated from the saturation regime using the formula $\mu_{FET} = 2I_{DS}L[WC_i(U_G - U_T)^2]^{-1}$, where C_i is the capacitance of the insulator per unit area (22 nF/cm^2), L and W are the channel length and width, respectively, and U_T is the threshold voltage obtained from the intercept with the X axis of a line drawn through the linear region in the plot $\sqrt{I_{DS}}$ versus U_G (see Figures 6b and 7b).[36] Disordered control samples prepared by drop-casting from hot toluene solution onto a heated (50 °C) substrate showed almost no drain-source current modulation for applied U_G. Preparation, AFM, and FETs measurements were performed in a clean room in normal atmosphere with dust-free air. FET measurements were quite reproducible after 2 months.

Acknowledgment. This work was partially financially supported through the EC Integrated Project NAIMO NMP4-CT-2004-500355, DGI Spain BQU2003-0760, Dursi Catalunya 2005SGR 00591, and MNiI Grant T08E 01327, Poland. We acknowledge the European Synchrotron Radiation Facility for provision of synchrotron radiation.

Supporting Information Available: Complete ref 7. This material is available free of charge via the Internet at http://pubs.acs.org.

CM060675M

(35) Shi, Z.; Enoki, T.; Imaeda, K.; Kazuhiko, S.; Wu, P.; Inokuchi, H.; Saito, G. *J. Phys. Chem.* **1988**, *92*, 5044.

(36) Newman, C. R.; Frisbie, C. D.; da Silva Filho, D. A.; Brédas, J. L.; Ewbank, P. C.; Mann, K. R. *Chem. Mater.* **2004**, *16*, 4436.